

PART - I

P A R T I

GENERAL INFORMATION ON SODIUM NITRATE AND CALCITE

AND

TECHNIQUES AND GRAPHICAL ANALYSIS

CHAPTER I

GENERAL INFORMATION ON
SODIUM NITRATE AND CALCITE

CHAPTER I

GENERAL INFORMATION ON SODIUM NITRATE AND CALCITE

	PAGE
1.1 INTRODUCTION ...	1
1.2 CRYSTALLOGRAPHY OF SODIUM NITRATE AND CALCITE	7
1.2.1 MILLER-BRAVAIS NOTATION ...	7
1.2.2 MILLER NOTATION FOR TRIGONAL CRYSTALS	8
1.2.3 CRYSTAL STRUCTURE ...	12
1.2.4 CLEAVAGE, GLIDING AND TWINNING ...	13
1.2.5 PERCUSSION MARK ...	14

FIGURES

REFERENCES

1.1 INTRODUCTION:

Sodium nitrate and calcium carbonate are isostructural and isomorphous. They are available in nature under the names of soda-niter (saltpetre) and calcite respectively. The size and perfection of these crystalline structures in general and particularly of calcite has attracted the attention of crystallographers. Looking to the availability of natural crystals of these two materials all over the world, the natural nitrates are few in number and are of rare occurrence whereas in the entire mineral kingdom, next to quartz, calcite crystals are more abundant, widespread, beautiful than any other species and exhibit probably the largest number of habits (about 700) and as a result played a prominent role in the history of mineralogy.

Chemically sodium nitrate and calcium carbonate belong to a group of salts known as oxysalts with a general formula AXO_3 . 'A' represents cation and XO_3 anion (X is carbon or nitrogen). Their structure types correspond to a member of the calcite group. Their bonding is basically ionic. There are several important characteristic features. For example, comparison of their structures with those of other oxysalts of the aragonite - structure type (AST) indicates that these materials with calcite structure type (CST) have relatively small cations 'A' where 'A' may be Li, Na, Mg, Ca, Fe, Zn, Co and Cd. The ASTs have large cations, 'A' (A = K, Ba, Sr, and Pb). A few compounds near the critical radius ratio of 0.73 between the two types are polymorphous. These include $CaCO_3$ and KNO_3 ; the lower temperature polymorphs crystallizing in the CST. In what follows $NaNO_3$ and $CaCO_3$ will mean sodium nitrate crystal and calcium carbonate crystal or calcite crystal. $NaNO_3$ and $CaCO_3$ possess extreme birefringence and optically negative character, exhibit perfect rhombohedral cleavages, gliding and twinning. However, there are differences between these materials for some other properties, e.g. in the binary series

between the members of the calcite group the available evidence indicates that complete series exists between CaCO_3 - MnCO_3 , FeCO_3 - MgCO_3 , FeCO_3 - MnCO_3 and probably between ZnCO_3 - MnCO_3 . Extensive series with small central gaps apparently extend between MgCO_3 - MnCO_3 and CaCO_3 - FeCO_3 and less extensive series between ZnCO_3 - CaCO_3 , ZnCO_3 - FeCO_3 , ZnCO_3 - MgCO_3 and CaCO_3 - MgCO_3 . These relations are predicted from the relative sizes of the ions involved, except that the series of ZnCO_3 with FeCO_3 and MgCO_3 should be complete. These features are not exhibited by NaNO_3 . Calcite is sparingly soluble in distilled water whereas NaNO_3 is highly soluble in water. However, solubility of NaNO_3 in water is more a chemical property than a physical one because it is an endothermic process whereas CaCO_3 is soluble to some extent in carbonated water leading to the formation of calcium bicarbonate as the end product. NaNO_3 undergoes lattice distortion at temperature approaching λ -transition. These being less than 2% change in volume/1/. The transition takes place reversibly over the range 150°C to 270°C/2/. It gradually changes from calcite structure to a closely similar one, still rhombohedral in which nitrate ions are essentially (but not strictly) disposed at random between two possible orientations α and β , differing by a 60° rotation about 3-fold axis. Its melting point is 308°C and decomposes at 380°C under atmospheric pressure. For calcite it is reported /71,73/ that it decomposes into calcium oxide (lime) and carbon dioxide at 850°C. However, by conducting studies on thermal etching of calcite cleavages in this laboratory, it is shown that the decomposition on microscopic scale starts, under atmospheric pressure, at about 500°C /3/. CaCO_3 melts at 1289°C under a pressure of 110 atmospheres. At the time of Second World War due to shortage of calcite, polarizing prisms of calcite were replaced by those of NaNO_3 . Since NaNO_3 is hygroscopic, precautions were taken to keep it free from moisture. Even then replacement was not found convenient. In view of the chemical and crystallographic importance of these materials, successful attempts were made to grow them in the form of synthetic single crystals. Thus NaNO_3 crystals were grown from melt /4-7/ and from solution /8/ whereas calcite crystals by solution growth /9-15/, crystal pulling /16/, Gel /17-21/, solvent zone melting

/22,23/ and hydrothermal growth /24/. NaNO_3 readily forms overgrowth upon calcite /25/*/. The crystal axes of the substances are usually parallel. Its growth and orientation on muscovite /26/*/, on dolomite /27/*/, on baryto-calcite /28/*/, on alkali halides /29/*/, on certain phenols /30/*/ and also upon NaNO_3 rhombohedra are well-known. Thermal and chemical dissolution of calcite under controlled conditions has been studied extensively /3,31-67/ by the workers in this laboratory and elsewhere. Excellent accounts are now available in several monograms, text-books and treatises /68-72/. Since CaCO_3 has many multifarious uses, several titles are now available /73-79/. The physical and chemical properties and mineralogical features are summarised in table 1-1.

TABLE 1.1

Physical and chemical properties and mineralogical features

Sr.No.		Sodium nitrate	Calcite
1.	Chemical formula /73/	NaNO_3	CaCO_3
2.	Molecular weight /73/, gm	85.0	100.1
3.	Molar volume /76/, cm^3 under atmospheric pressure	41.9	36.934
4.	Solubility /73/, g/100g of water at 20°C	88	0.0065
5.	Colour /73,75,78,79/	Colourless, White, Brown, Lemon yellow; Green	Colourless, white, Red, Blue, Violet, Green, Yellow
6.	Specific gravity /73/	2.26	2.93
7.	Melting point under atmospheric pressure /73/, °C	308	850 (dissociates)
8.	Boiling point under atmospheric pressure /73/ °C	380 (dissociates)	-

Sr.No.	Sodium nitrate	Calcite	
9.	Phase transformation /77/ °C	150 to 273	-
10.	Hardness /75/, on Mho's scale	1.5 to 2	3
11.	Elastic constants /74/ (Elastic coefficients, bars) at 27°C	C ₁₁ : 8.67 C ₁₂ : 1.63 C ₁₃ : 1.60 C ₃₃ : 3.74 C ₄₄ : 2.13	C ₁₁ : 13.71 C ₁₂ : 4.56 C ₁₃ : 4.51 C ₃₃ : 7.97 C ₄₄ : 3.42
12.	Elastic Moduli /74/: ₂ Young's Modulus, dynes/cm	-	7.24 x 10 ¹¹ (parallel) 8.825 x 10 ¹¹ (perpendicular)
	: Bulk Modulus	2.619 x 10 ¹¹	1.296 x 10 ¹²
13.	Specific heat /74/, g-cal/g(15°)		
	: at 0°C	0.247	0.203
	: at 100°C	0.270	0.214
14.	Thermal conductivity /74/, cal/cm-s-°C		
	: at 0°C	-	0.0132
	: at 100°C	-	0.0111
15.	ΔH - Heat of formation /78/ at 18°C, kg-cal/mol., -ve values indicate heat is evolved in the process of formation	- 111.72	- 289.1
16.	ΔF - Free energy of formation /78/, at 25°C, kg-cal/mol.	-	- 207.22
17.	Dielectric constant /76/	2.18	-
18.	Electrical conductivity /76/, Mho's		
	: at 52°C	0.662 x 10 ⁻¹²	-
	: at 200°C	0.176 x 10 ⁻⁷	-
	: at 289°C	0.155 x 10 ⁻⁴	-
19.	Velocity of sound in inorganic solids at room temperature /73/ (longitudinal velocity) km/sec	5.31	6.45

Sr.No.		Sodium nitrate	Calcite
20.	Refractive index n_D /62/	O : 1.5874 E : 1.3361	O : 1.65838 E : 1.48645
21.	Optic axis /74/	[111]	[111]
22.	Birefringence /75/	negative	negative
23.	<u>Crystallographic data:</u> /75,78,79/		
(i)	System ..	Hexagonal (Trigonal)	Hexagonal (Trigonal)
(ii)	Class ..	$\bar{3} \frac{2}{m}$	$\bar{3} \frac{2}{m}$
(iii)	Space group ..	R $\bar{3} C$	R $\bar{3} C$
(iv)	Lattice parameters	a:c :: 1:0.8276 $\alpha = 102^\circ 46\frac{1}{2}'$	a:c :: 1:0.8543 $\alpha = 101^\circ 55'$
(v)	Unit cell ..	Rhombohedral	Rhombohedral
(vi)	Symmetry ..	Rhombic	Rhombic
(vii)	Cleavage ..	{1011} perfect	{1011} perfect
(viii)	Fracture ..	Conchoidal, but seldom observable	Conchoidal, but difficult to produce
(ix)	Elasticity ..	Sectile	Brittle
(x)	Lustre ..	Vitreous	Vitreous to earthy
(xi)	Fusibility ..	Fusible (degree 1)	Infusible
(xii)	Solubility ..	Soluble in H ₂ O	Soluble in HCl
(xiii)	Special properties	Deflagrates, diamagnetic	Glows under (before blow pipe) some variety fluoresce. red; pink; photoluminescent

Sr.No.		Sodium nitrate	Calcite
(xiv)	Locality (chief)	Northern Chile, Nevada, California	Abundant worldwide, optical, Pedro mountains, Northern Mexico
(xv)	Habit	Rhombohedral crystals, similar to those of calcite, are uncommon. Usually granular, encrusting or efflorescent.	Prismatic, scalenohedral, rhombohedral, tabular, or acicular, often twinned. Also massive, cleavable, oolitic, stalactitic, granular or earthy.
(xvi)	Structure cell, cell content	$\text{Na}_2(\text{NO}_3)_2$ in the rhombohedral unit	$\text{Ca}_2(\text{CO}_3)_2$ in the rhombohedral unit
(xvii)	Streak	Colourless	White to colourless
(xviii)	Diaphaneity	Transparent to translucent	Transparent to opaque
(xix)	Effervescence	-	Freely in dilute acids
(xx)	Occurrence and mineral associations	As a surface deposit in arid regions. Associated minerals include niter, gypsum and halite.	Common in sedimentary rocks; of hydrothermal origin in some basic rocks; a primary con- stituent of some alkaline rocks; vein deposits; replacement materials in some fossils; skeletal materials of some past and present organisms. Mineral associates are too numerous to mention.
(xxi)	Uses	Fertilizer, also noted in the manu- facture of nitric acid and potassium nitrate.	Cements, optical equip- ment, chalk, rubber filler, putty, paint and metallurgy.
(xxii)	Other names	Soda niter, saltpetre	-
(xxiii)	Secondary names	-	Calc-spar, dogtooth spar, nailhead spar, Iceland spar.
(xxiv)	Artificial growth	From solution /8/ and melt /4-7/	From solution /9-15/ by crystal pulling /16/ in gel /17-21/, solvent zone melting /22,23/ hydrothermal growth /24/.

1.2 CRYSTALLOGRAPHY OF SODIUM NITRATE AND CALCITE:

Sodium nitrate and calcium carbonate belong to a hexagonal system with class $\bar{3} 2/m$ and space group $R\bar{3}C$. Some crystallographers prefer to group the above to a trigonal (rhombohedral) system. There is now a tendency to group all the classes of these two systems (hexagonal and trigonal) together in sub-divisions of one larger hexagonal system. The full symmetry of the rhombohedral crystals of calcite group consists of the following: (1) centre of symmetry (2) one triad axis (3) three diad axes (4) three planes of symmetry. The crystallographic axes for this system are in terms of either Miller-Bravais axial scheme or Miller scheme alone /80/.

1.2.1 Miller-Bravais Notation:

Three vertical diagonal planes of symmetry meet in the triad axis, and normal to these three planes are three horizontal principal axes of 2-fold symmetry which, in the Miller-Bravais notation, are the axes a_1 , a_2 and a_3 , the C-direction being parallel to the vertical axis of 3-fold symmetry. The three axes are coplanar and inclined at an angle of 120° with each other. The three directions are all of equal significance. These crystals are thus described in terms of four crystallographic axes (Fig.1.1), namely three horizontal axes $a_1(H)$, $a_2(H)$ and $a_3(H)$ at an angle of 120° to each other and normal to the vertical axis, $C(H)$. The diad axes chosen as the $a_2(H)$ direction runs horizontally to the right, $+a_1(H)$ direction runs upwards towards the left and $+a_3(H)$ downwards towards the left. The direction $C(H)$ is ofcourse normal to the plane of axes $a_1(H)$, $a_2(H)$ and $a_3(H)$; it is also the intersection of the polar edges of crystallographically fundamental cleavage rhombohedron of this group. The general symbol of the form is $h\bar{o}hl$, such as $10\bar{1}1$, normal to one of the vertical planes of symmetry. The operation of the triad axis gives only three such faces $10\bar{1}1$, $\bar{1}101$ and $0\bar{1}11$ on top (or above) and the operation of the centre (or of the horizontal diads) gives three parallel faces $\bar{1}01\bar{1}$, $1\bar{1}0\bar{1}$ and $01\bar{1}\bar{1}$ below (or down). There are no faces of this form symmetrically below the upper faces. This is obvious from the stereogram

of the form $\{10\bar{1}1\}$ of a holosymmetric trigonal crystal (Fig.1.2). The forms $\{h\bar{o}hl\}$ constitute a family of rhombohedra which become more and more acute as the ratio $h:l$ becomes larger. In terms of the lengths of the axes a and C , the rhombohedrons become more and more flattened or obtuse with the decrease of C -axes and vice versa. A cube placed with an octahedral axis vertical is obviously the limiting case between the obtuse and the acute forms where the interfacial angle is 90° .

Various nomenclatures have been introduced to differentiate a rhombohedron such as $\{10\bar{1}1\}$ or $\{h\bar{o}hl\}$ (Fig.1.3) from its geometrically similar complementary rhombohedron $\{01\bar{1}1\}$ or $\{ok\bar{k}l\}$ (Fig.1.4). Thus one is termed a positive rhombohedron with an upper face towards the observer and the other a negative rhombohedron, with an edge towards the observer, but this mode of distinction seems specially undesirable in view of the established usage of +ve and -ve in optical work. Direct and inverse or obtuse and reverse are more satisfactory terms, but not widely used. The stereogram of this holosymmetric trigonal crystal is shown in Fig.1.5 (a).

1.2.2 Miller Notation for Trigonal Crystals:

Instead of using a four-index notation for describing a trigonal crystal, it is possible to use a three-index notation. In this case the crystallographic axes are parallel to the three polar edges of the fundamental (unit) rhombohedron usually described by $\langle 10\bar{1}1 \rangle$ in Miller-Bravais notation. It should be noted here that these axes are not parallel to symmetry axes and selection of axes is not in tune with the guidelines of the law of rational indices. The axes are equally inclined to the triad axes and are non-orthogonal, but make equal angles with each other; this angle between the axes is the plane angle of the face of the rhombohedron (not the crystallographic interfacial angle) and it depends upon the shape of the rhombohedron in the particular substance in question. Instead of a characteristic axial ratio for each substance, a characteristic angle α is given in this method of description.

The crystals are still set up as before with the triad axis vertical, and are projected on a plane normal to the triad axis. Since the edges of the fundamental rhombohedron define the directions of the crystallographic axes, the indices of the three upper faces must be 100, 010 and 001 (Fig.1.1). Note that the three axes do not emerge through the poles of these faces, since they are parallel to the edges and not to face normals. The points of emergence of the axes a_1 , a_2 and a_3 can be located in the projection by finding the poles of the zones 010 - 001, 001 - 100 and 100 - 010 respectively. Since the three axes are equally inclined to the plane of projection, the Miller indices of the forms described in the Miller-Bravais notation can easily be determined. It should be remarked here that this (Miller) notation is not used for truly hexagonal crystals as it creates serious misunderstanding while labelling adjacent faces of a single form, say hexagonal bipyramid.

It may sometimes be necessary to connect an index pqr of a face in Miller notation to the corresponding index hkil in Miller-Bravais notation or vice versa. This is readily accomplished on a stereogram (Fig.1.5(b)) by adopting the convention that the particular face 100 in one notation shall always be indexed $10\bar{1}1$ in the other. The tables 1.2 and 1.3 present conversion tables for Indices of planes and Indices of directions.

TABLE 1.2

(a) Conversion table for indices of planes

Face x with Miller-Bravais indices (hkil) and Miller indices (pqr) where

$$(1) \quad h = p - q, \quad k = q - r, \quad i = r - p, \quad l = p + q + r$$

$$(2) \quad p = h - i + l, \quad q = k - h + l, \quad r = i - k + l$$

(b) Conversion table for indices of direction

Transformation relation between the indices of a direction [x y z] and [u v t w] when referred to the system of axes $a_1(R)$, $a_2(R)$ & $a_3(R)$ and $a_1(H)$, $a_2(H)$, $a_3(H)$ & $c(H)$, respectively, as

$$u = \frac{2x - y}{3}, \quad v = \frac{2y - x}{3}, \quad t = -(u + v), \quad w = z.$$

Also note

$$x = u - t, \quad y = v - t \quad \text{and} \quad z = w.$$

The table 1.3 describes the standard forms/family of planes in Miller-Bravais notation and Miller notation whereas table 1.4 describes the transformation of Miller Indices to Miller-Bravais Indices of some prominent/major planes in rhombohedral crystals.

TABLE 1.3

Standard forms/family of planes of holosymmetric trigonal crystal (calcite) in Miller-Bravais and Miller notation

Form/Family of Planes	Miller-Bravais Notation	Miller Notation
Basal Pinacoid	{0001}	{111}
Hexagonal Prisms	{10 $\bar{1}$ 0}	{2 $\bar{1}$ $\bar{1}$ }
	{11 $\bar{2}$ 0}	{10 $\bar{1}$ }
Dihexagonal Prisms	{hkio}	
Rhombohedron: Positive	{ho \bar{h} l}	
	{10 $\bar{1}$ 1}	{100}
Negative	{ok \bar{k} l}	
	{01 $\bar{1}$ 1}	{22 $\bar{1}$ }
Ditrigonal Scalenohedron	{hkil}	{pqr}

TABLE 1.4

Table of transformation of Miller indices (MI) to Miller-Bravais indices (MBI) of some prominent/major planes in rhombohedral crystals

MI	MBI	MI	MBI
100	$10\bar{1}1$	$\bar{1}\bar{1}2$	$0\bar{1}10$
010	$\bar{1}101$	$1\bar{2}1$	$1\bar{1}00$
001	$0\bar{1}11$	$11\bar{1}$	$02\bar{2}1$
110	$01\bar{1}2$	$\bar{1}11$	$\bar{2}021$
011	$\bar{1}012$	$1\bar{1}1$	$2\bar{2}01$
101	$1\bar{1}02$	$20\bar{1}$	$21\bar{3}1$
111	0001	$02\bar{1}$	$\bar{2}3\bar{1}1$
$10\bar{1}$	$11\bar{2}0$	$\bar{1}20$	$\bar{3}211$
$01\bar{1}$	$\bar{1}2\bar{1}0$	$\bar{1}02$	$\bar{1}231$
$\bar{1}10$	$\bar{2}110$	$0\bar{1}2$	$1\bar{3}21$
$\bar{1}01$	$\bar{1}\bar{1}20$	$2\bar{1}0$	$3\bar{1}\bar{2}1$
$0\bar{1}1$	$1\bar{2}\bar{1}0$	310	$21\bar{3}4$
$1\bar{1}0$	$2\bar{1}\bar{1}0$	130	$\bar{2}3\bar{1}4$
$2\bar{1}\bar{1}$	$10\bar{1}0$	031	$\bar{3}214$
$11\bar{2}$	$01\bar{1}0$	013	$\bar{1}234$
$\bar{1}2\bar{1}$	$\bar{1}100$	103	$1\bar{3}24$
$\bar{2}11$	$\bar{1}010$	301	$3\bar{1}\bar{2}4$

1.2.3 Crystal structure:

The crystal structures of NaNO_3 and CaCO_3 are almost similar. The calcite structure was one of the earliest studied by X-rays in 1914 by Bragg /81/. Its optical properties were derived in terms of the atomic structure. In the Fig. 1.6 calcium (or sodium) atoms are represented by blank circles, carbon (or nitrogen) atoms by lined circles and oxygen atoms by black circles. The calcite lattice may be regarded as a deformed rocksalt lattice. The later is stood on a diagonal (looked at from above in the Fig.1.6(a)), all the Na^+ ions replaced by Ca^{++} (or Na^+ in NaNO_3) ions and all the Cl^- ions by CO_3^{--} (or NO_3^-) ions, consisting of central carbon (or nitrogen) atoms surrounded by an equilateral triangle of oxygen atoms in a plane at right angles to diagonal, i.e. the plane of the paper. On account of the space occupied by these ions, the cube expands in a horizontal direction and forms the cleavage rhombohedron of calcite (or sodium nitrate), calcium (or sodium) and carbon (or nitrogen) atoms are spaced at equal intervals along the crystal axes. However there is a little difference between the orientation of CO_3^{--} and NO_3^- ions. The carbonate ions are having a more planar structure than that of nitrate ions. In case of CO_3^{--} ions, the distances between central carbon atom to oxygen atom is 1.23 \AA while side of equilateral triangle, made by oxygen atoms, has a length of 2.13 \AA . For NO_3^- ions, the distance between central nitrogen to oxygen atom is 1.21 \AA and the distance between any two oxygen atoms is 2.108 \AA .

The lattice constants of these trigonal crystals are as follows:

	<u>Sodium nitrate</u>	<u>Calcite</u>
a	5.07 \AA	6.36 \AA
c	16.81 \AA	17.02 \AA
α	$102^\circ 46\frac{1}{2}'$	$101^\circ 55'$

In the rhombohedral unit cell, the content is 2 molecules of each for the above.

1.2.4 Cleavage, Gliding and Twinning:

Sodium nitrate and calcite exhibit perfect rhombohedral cleavage $\{10\bar{1}1\}$, a cleavage in three directions at oblique angles to each other and are susceptible to abrasion or scratching. In case of calcite some crystals exhibit cleaved areas upto 0.2 x 0.2 mm free from cleavage lines. Over such an area the crystals appear to have cleaved true to a single molecular plane (Tolanski and Khamasavi, 1946) /82/. Both crystals sometimes exhibit parting parallel to $\{01\bar{1}2\}$, $\{10\bar{1}2\}$ and $\{0001\}$. Fracture is conchoidal but seldom observable, since the crystals are brittle. NaNO_3 is softer than CaCO_3 ; their hardness on Moh's scale are 1 and 3 respectively. This property varies on different planes and in different directions.

The phenomenon of twinning occurs in almost identical fashion in both these crystals. In view of the enormous uses and availability of calcite, this feature is studied in much more detail for calcite than for sodium nitrate. The following rules are found to be observed:

- (1) Twin plane $\{02\bar{2}1\}$ is rare with composition plane $\{02\bar{2}1\}$; sometimes it occurs on aggregates of a few individuals.
- (2) Twin plane $\{0001\}$ as the composition surface. Re-entrant angles are about the equator of the crystal except when bound laterally by $\{10\bar{1}0\}$. Twinning is then revealed by cleavage or by the apparent horizontal plane of symmetry.
- (3) Twin plane $\{10\bar{1}1\}$ is not common with composition surface $\{10\bar{1}1\}$. The twinned individuals have their axes nearly at right angles and also have a cleavage plane in common.
- (4) Twin plane $\{01\bar{1}2\}$ is very common with $\{01\bar{1}2\}$ as the composition face. This is often known as polysynthetic twinning with striations parallel to the long diagonal of the rhombohedral cleavage plane.

Sodium nitrate exhibits twin-gliding with $K_1\{10\bar{1}2\}$, $K_2\{0\bar{1}11\}$. The percussion figure on cleavage planes of NaNO_3 and CaCO_3 are almost identical.

1.2.5 Percussion mark:

Whenever a dull conical point, kept on a crystal face, is given a sharp quick blow, a figure is usually formed. This figure is known as a percussion mark. It can also be produced by allowing the impact of a solid polished steel sphere on the crystal surface (Raman, 1959) /83/. The formation of figure with the attendant features on a surface is a characteristic property of the crystal itself and is related to the structure of the crystal and to the orientation of the face on which the impact occurs. The study of percussion figure on a crystal surface is important in revealing the effect of concentrated stress and its propagation in and around the crystal face under consideration.

When a percussion figure produced on a cleavage face of sodium nitrate (Fig.1.7a) or calcium carbonate (Fig.1.7b) was examined under a microscope, it was observed that on either side of the area of contact between the dull conical point (or impinging sphere) and the crystal surface, two cleavage lines (or a number of pairs of cleavage lines) making an obtuse angle 102° with each other developed and extended outwards from the edge of that area (Fig.1.8). These lines are clearly visible on the face of the crystal and they sharply limit the area within which fracture develops. Another interesting feature is the appearance of a whole series of parallel lines outside the region of contact and only on one side of it. These lines are equally inclined to the two sets of cleavage lines and may be explained as being due to glides occurring within the crystal along the direction of a rhombohedral edge. The percussion figure with the point of impact as the vertex of the triangle formed by the two cleavage lines and the series of parallel lines is oriented oppositely with respect to that corner of the crystal, where three obtuse angles

meet. The line which is perpendicular to the series of parallel lines and passing through the vertex of the triangle has the direction [110] which is also the line of symmetry for the cleavage surface and percussion mark. Sometimes interference colours are also observed between the thin cleavage flake (through the air gap produced) and the main cleavage surface; the flake and the surface being loosely attached to each other through the air gap produced by the impact. This effect can be minimised by taking adequate precautions while impinging the crystal surface by a dull point. The percussion figures can be utilized to determine the orientation of etchpits and their boundaries. The line diagram on a cleavage plane of rhombohedral crystals showing the above features of percussion mark is given in Fig.1.8.

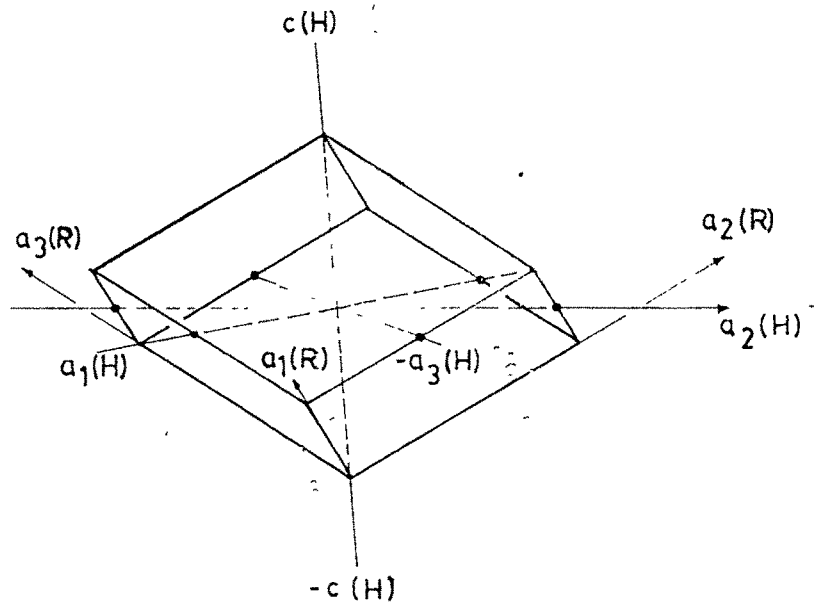


Fig.1.1 Positive unit rhombohedron $\{10\bar{1}1\}$ with axes $a_1(H)$, $a_2(H)$, $a_3(H)$ and $C(H)$ in Miller-Bravais notation and $a_1(R)$, $a_2(R)$ and $a_3(R)$ in Miller notation. In hexagonal system with four-index notation, the three horizontal coplanar axes $a_1(H)$, $a_2(H)$ and $a_3(H)$ are inclined at an angle of 120° with each other and vertical axis $C(H)$ is normal to the plane of the three coplanar axes. The diad axis $+a_2(H)$ runs horizontal to the right, $+a_1(H)$ direction downwards towards the left and $+a_3(H)$ direction upwards towards the left. In terms of the three-axes notation, the axes $a_1(R)$, $a_2(R)$ and $a_3(R)$ are parallel to the edges of the fundamental rhombohedron.

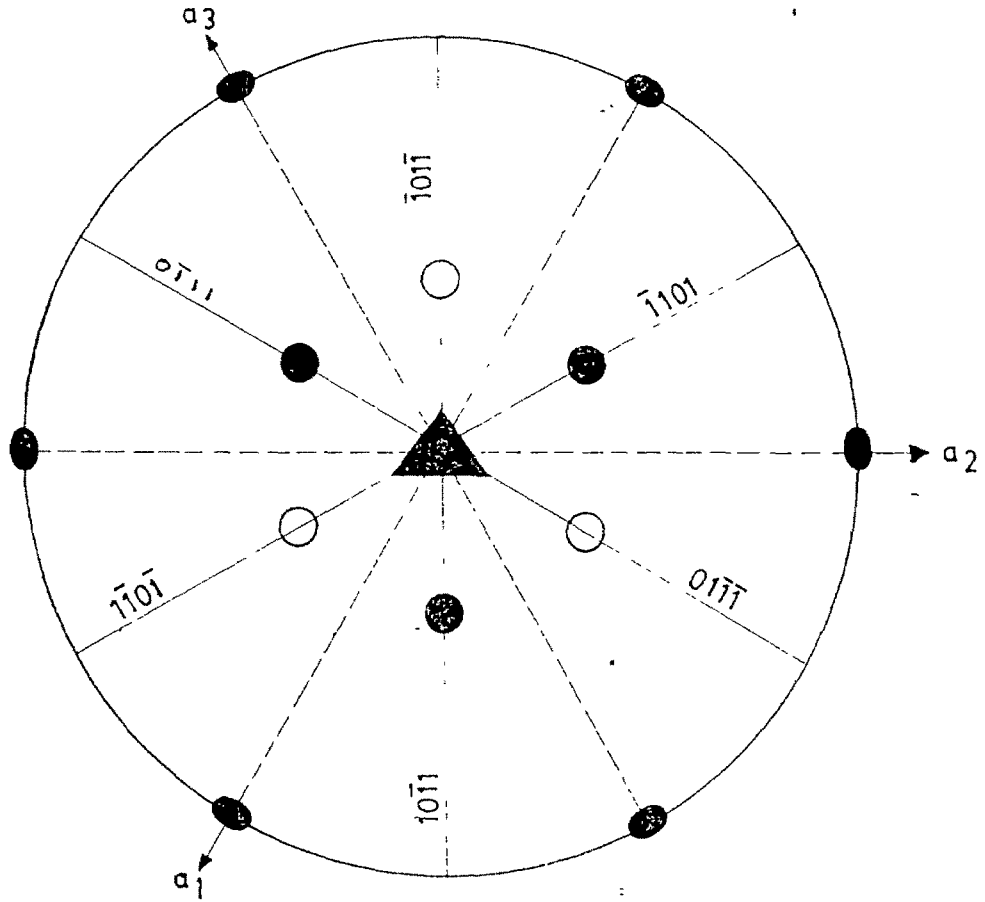


Fig.1.2 Stereogram of the form $10\bar{1}1$ of a holosymmetric trigonal crystal. The operation of triad axis gives three faces $10\bar{1}1$, $\bar{1}101$ and $0\bar{1}11$ shown by black circles and that of the centre (or of the horizontal diads) three faces $\bar{1}0\bar{1}\bar{1}$, $1\bar{1}0\bar{1}$ and $01\bar{1}\bar{1}$ shown by open circles.

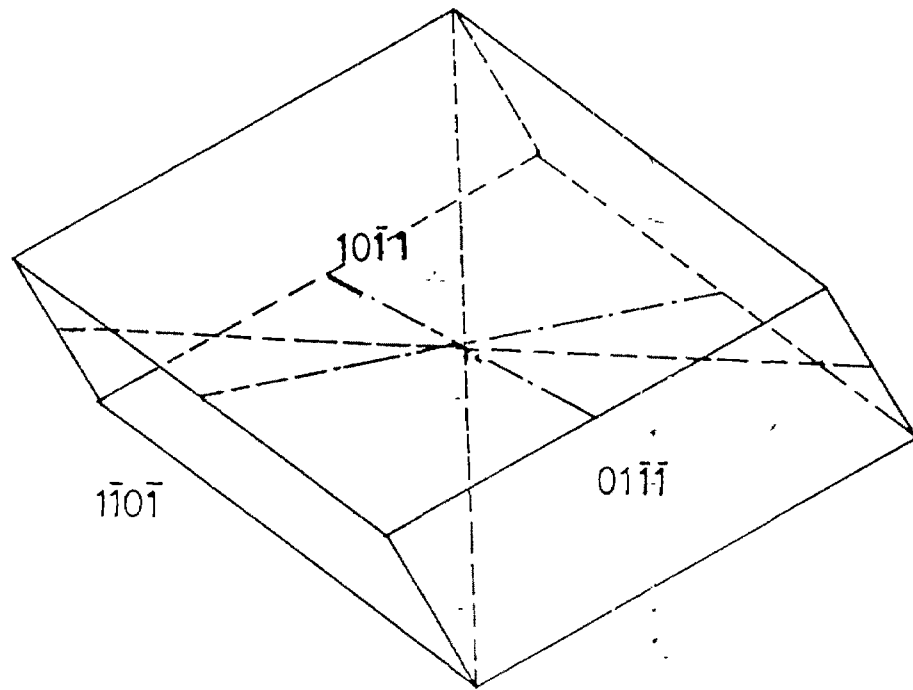


Fig.1.3 Unit positive rhombohedron $\{10\bar{1}1\}$ with axes in Miller-Bravais scheme.

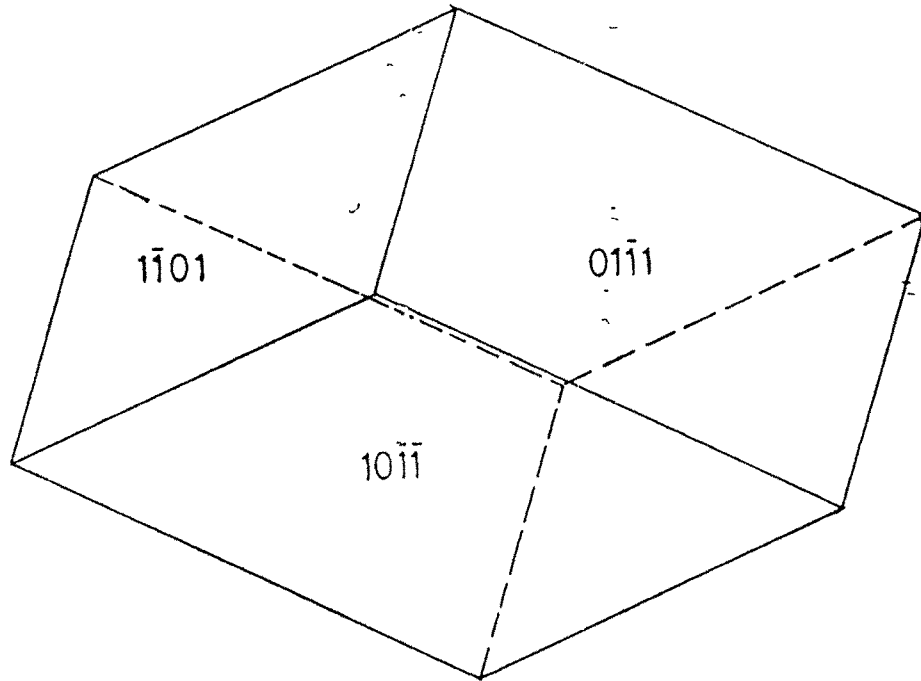


Fig.1.4 Negative fundamental rhombohedron $\{10\bar{1}\bar{1}\}$.

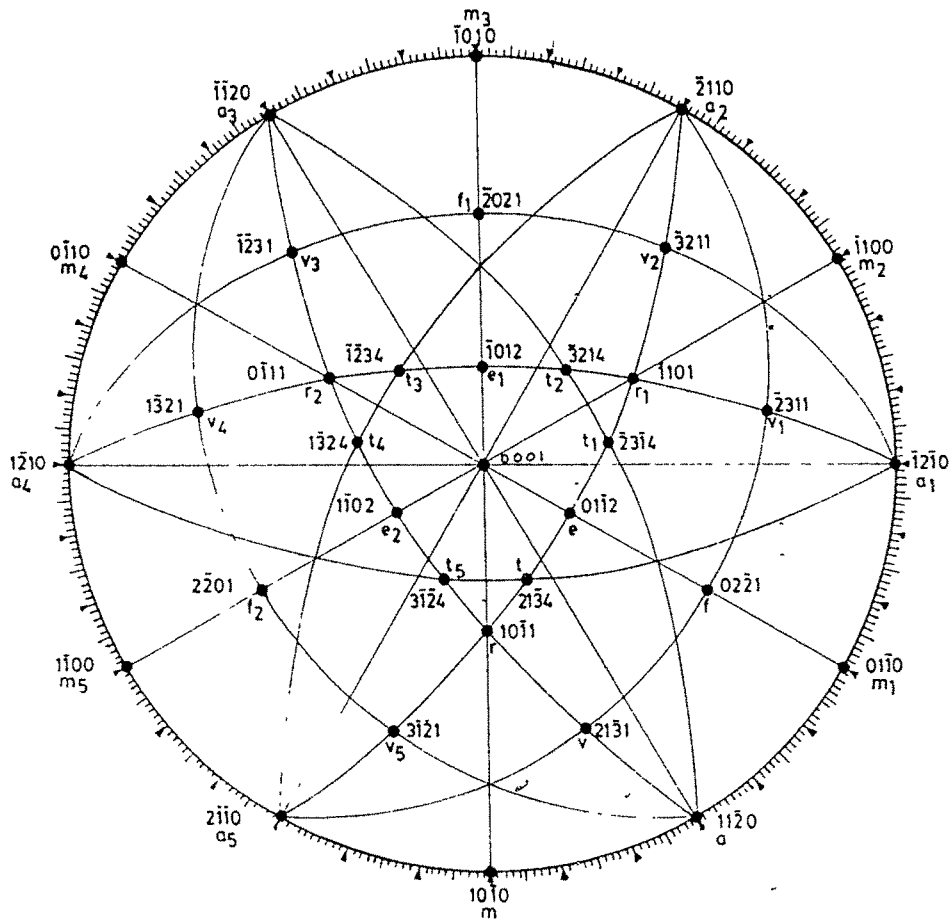


Fig.1.5(a) Stereogram on a basal plane (0001) of a typically complex crystal of calcite, showing the symmetry in the distribution of faces. Forms in Miller-Bravais notation are-

- (i) Prisms $\{11\bar{2}0\}$
(six faces a, a_1, a_2, a_3, a_4 & a_5)
- (ii) Prisms $\{10\bar{1}0\}$
(six faces m, m_1, m_2, m_3, m_4 & m_5)
- (iii) Positive rhombohedrons $\{10\bar{1}1\}$
(three faces r, r_1 & r_2)
- (iv) Negative rhombohedron $\{01\bar{1}2\}$ and $\{02\bar{2}1\}$
(three faces in each: e, e_1 & e_2 ; f, f_1 & f_2)
- (v) Scalenohedron positive $\{21\bar{3}1\}$ and $\{21\bar{3}4\}$
(six faces in each: v, v_1, v_2, v_3, v_4 & v_5 ;
 t, t_1, t_2, t_3, t_4 & t_5)

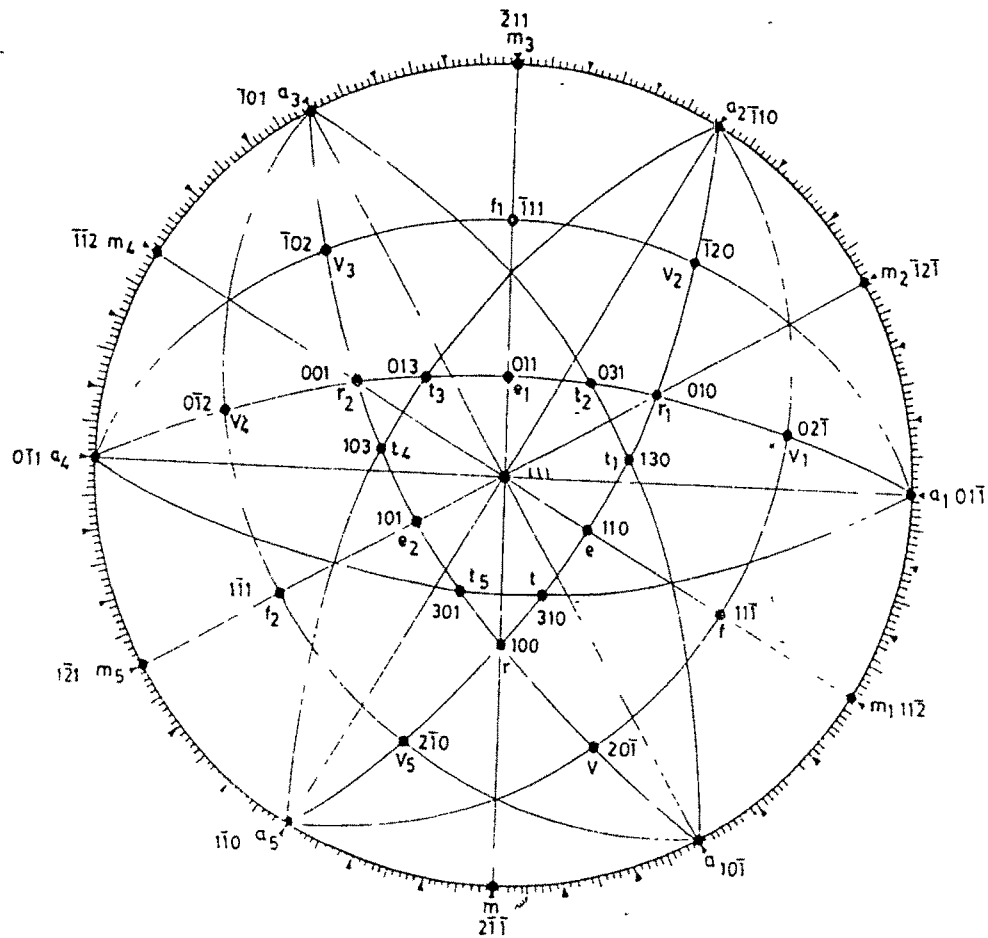


Fig.1.5(b) Stereogram on a plane (111) of a typically complex crystal of calcite, showing the symmetry in the distribution of faces. Forms in Miller notation are-

- (i) Prisms $\{10\bar{1}\}$
(six faces a, a_1 , a_2 , a_3 , a_4 & a_5)
- (ii) Prisms $\{2\bar{1}\bar{1}\}$
(six faces m, m_1 , m_2 , m_3 , m_4 & m_5)
- (iii) Positive rhombohedrons $\{100\}$
(three faces r, r_1 & r_2)
- (iv) Negative rhombohedrons $\{110\}$ and $\{11\bar{1}\}$
(three faces in each: e, e_1 & e_2 ; f, f_1 & f_2)
- (v) Scalenohedron positive $\{20\bar{1}\}$ and $\{310\}$
(six faces in each:
v, v_1 , v_2 , v_3 , v_4 & v_5 ; t, t_1 , t_2 , t_3 , t_4 & t_5)

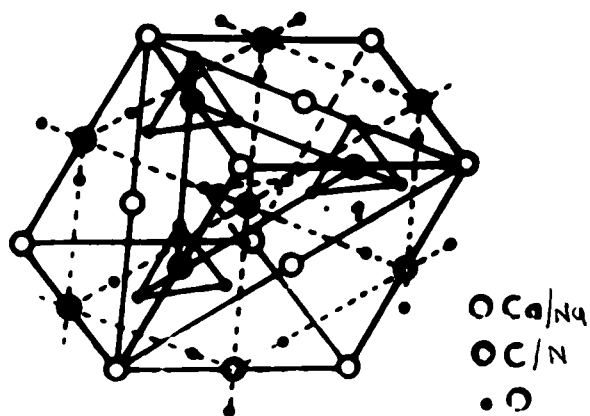


Fig.1.6 Crystal structure of calcite (or sodium nitrate).

The calcite (or sodium nitrate) lattice, with calcium (or sodium) atoms by black circles, carbon (or nitrogen) atoms by lined circles and oxygen atoms by small black circles.

Distance between

C - O	:	1.23 A°
O - O	:	2.13 A°
N - O	:	1.21 A°
O - O	:	2.108A°

Lattice parameters

for CaCO ₃	:	a : 6.36 A°
		c : 17.02A°
for NaNO ₃	:	a : 5.07 A°
		c : 16.81A°

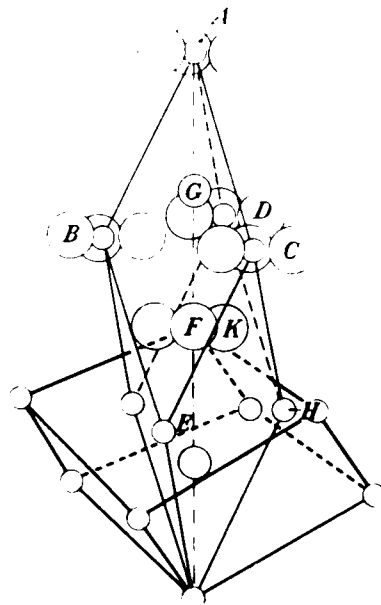


Fig.1.6(a) A drawing showing the relation between correct unit rhombohedron of the sodium nitrate (or calcite) arrangement and its cleavage rhombohedron. The bimolecular unit is the elongated cell, the cleavage pseudocell is that outlined by thick lines. Small circles at the corners are nitrogen (or carbon) atoms. Big circles are oxygen atoms.

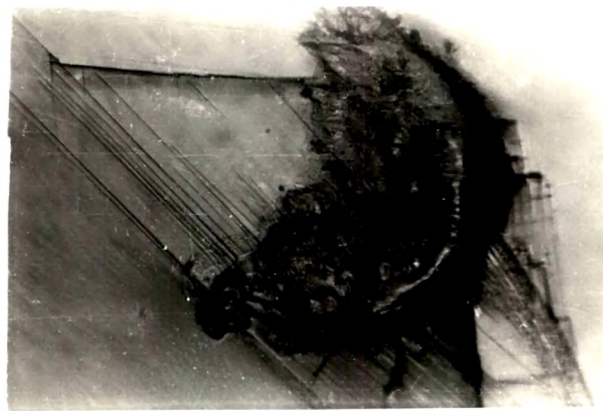


Fig.1.7(a) Percussion mark on cleavage face of synthetic single crystal of sodium nitrate (showing two cleavage lines making an obtuse angle 102° with each other, extending outwards from the edge of the indented area and appearance of a series of parallel lines outside the region of contact and only on one side of it. The lines are equally inclined with the cleavage lines).

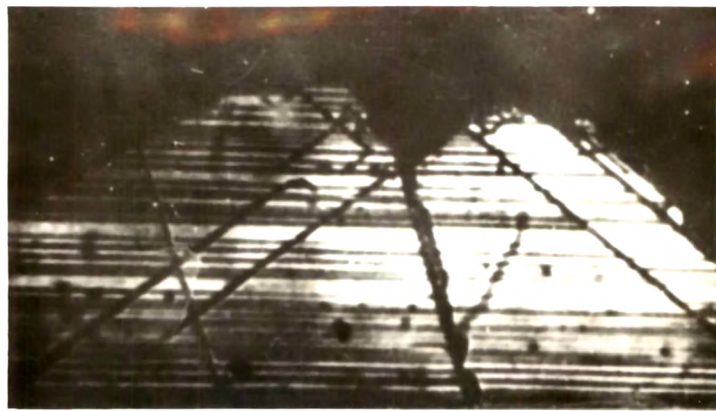


Fig.1.7(b) Percussion mark on cleavage face of natural calcite crystal, which is lightly etched by a concentrated solution of sodium sulfate.

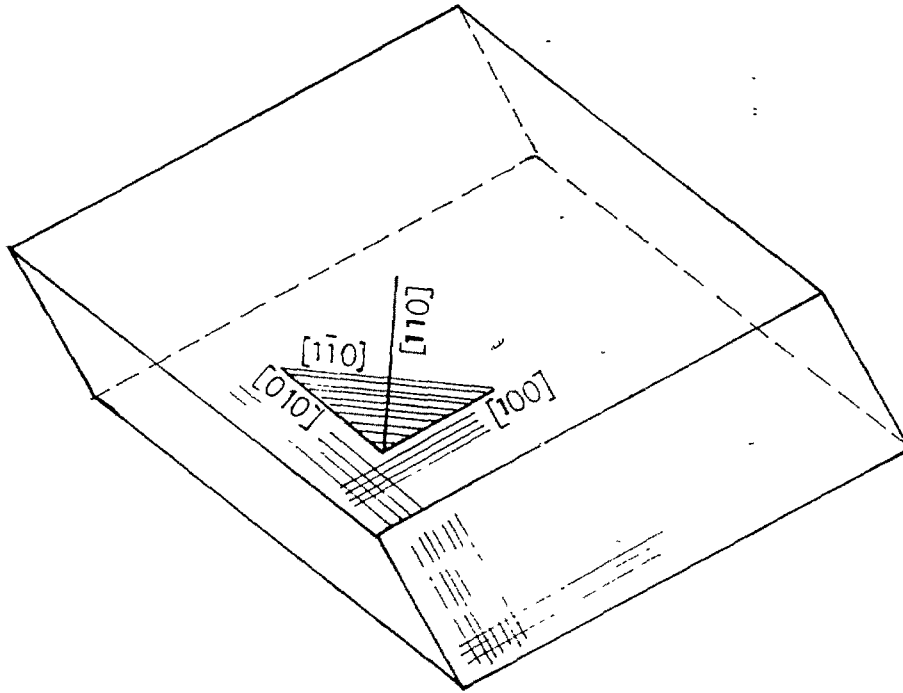


Fig.1.8 Two cleavage lines with directions $[100]$ and $[010]$ making an obtuse angle 102° with each other are present. Also, series of parallel lines with direction $[1\bar{1}0]$ which are equally inclined to the two sets of cleavage lines are present. These make a triangle. A line of symmetry perpendicular to $[1\bar{1}0]$ direction is $[110]$.

REFERENCES

1. M. Kantola & E. Vilhonen, Am. Acad. Sci. Fennicae, A.VI, 54, (1960).
2. A. Mustojoki, J. of Mat. Sci. A.VI No.5, 305, (1957).
3. B.J. Mehta, Ph.D. Thesis, The Maharaja Sayajirao University of Baroda, Baroda (1973).
4. Stober, F., Zs. Kr. 61, 315, (1925).
5. West, C.D., J. Opt. Soc. Amer. 35, 26, (1945).
6. F. Yamaguti, J. Phys. Soc. Japan, 7, 113, (1952).
7. S.N. Komnik & V.L. Startsev, J. Cryst. Growth (Netherlands), Vol 5, No.3, 207, (1969).
8. A. Holden & P. Singer, 'Crystals and Crystal Growing', Doubleday and Co., Inc., N.Y. (1965).
9. N. Yu. Ikornikva, Growth of Crystals (New York: Consultants Bureau), Vol 3, 297, (1962).
10. P.M. Gruzensky, Proceeding International Conference on Crystal Growth, Boston, 1966, J. Phy. Chem. Solids, (GB), Supp., No.1, 365, (1967).
11. G.K. Kirov, L. Filizova, I. Yesselinov. Acta Cryst. (Interact); Vol 925, pts.3, p.s.240. (1969). (Eighth International Congress of the International Union of Crystallography, Buffalo, Stony Brook and Upton, N.Y.; 7-24 Aug. 1969).
12. G.H. Nancollas, M.M. Reddy, J. Colloid & Interface Sci., (USA), Vol 37, No.4, 824, (1971).
13. G.K. Kirov, I. Vesselinov; Z. Cherneva. Kristall & Tech. (Germany), Vol 7, No.5, 497, (1972) In English.
14. H.M. Liaw, J.W. Faust. 2nd National Conference on Cryst. Growth (abstract only), Princeton, N.J., USA 30 July-3 Aug., (1972), (USA: American Assoc. Cryst. Growth 1972).
15. Jokichi Noda, J. Soc. Chem. Ind. Japan, 37, Suppl. binding 319, (1934).
16. J. Zemlicka. Acta Cryst. (Internat), Vol 21, pt.7, Suppl. A 264, (1966) [7th International Congress and Symposium International Union of Crystallography, Moscow 1960] In German.

17. H.J. Nickl, H.K. Henisch. J. Electrochem Soc. (USA), Vol 116, No.9, 1258, (1969).
18. C. Barta; J. Zemlicka, J. Crystal Growth (Netherlands), Vol 10, No.2, 158 (1971).
19. A. Schwartz, D. Eckart, K. Francis, Mater. Res. Bucl. (USA), Vol 6, No.12, 1341 (Dec 1971).
20. V.A. Bekunov, Kino - Foto - Khim - Prom 1937, No.8, 46, Khim - Referat - Zbur - F, No.7, 77 (1938).
21. H.W. Morse and J.D. Donnay, Bull. Soc. Franc. mineral; 54, 19 (1931).
22. J.J. Brissot, C. Belin. J. Cryst. Growth (Netherlands), Vol 8, No.2, 213 (1971).
23. C. Belin, J.J. Brissot, R.E. Jesse. J. Cryst. Growth (Netherlands), Vol 13-14, 597 (1972)[3rd International Conference on Crystal Growth, Marseilles, France, 5-9 July 1971].
24. J.F. Balascio, W.B. White. Mater. Res. Bull (USA), Vol 7, No.12, 1461 (1972).
- 25.* G. Finch & Whitmore. Trans. Faraday Soc. 34, 640, (1939); Barker, Trans. Chem. Soc., London, 89, 1123 (1906); Settele, Jb. Min., Beil. -Bd., 61, 227 (1930).
- 26.* Mugge, Cbl. Min; 355 (1902), Jb. Min; Beil.-Bd; 16, 389 (1903).
- 27.* Tschermark. Min. Mitt., 4, 118 (1882).
- 28.* Kreutz. Min. Mag., 15, 233 (1909),
- 29.* Royer. C.R., 205, 1418 (1937); Heintze; Zs. Kr., 97, 241 (1937).
- 30.* Willems. Zs. Kr., 105, 53 (1943).
31. A.J. Shah, J.R. Pandya. Crystal Res. Technol. 20, (1985), 6, 813.
32. L.J. Bhagia, J.R. Pandya. Crystal Res. & Techol. 18, (1983), 11, 1353.
33. J.R. Pandya, L.J. Bhagia. Surface Technology, 19, (1983) 187.

* Quoted in "Dana's System of Mineralogy" VIIth ed. Vol II, Ref.No.7 to 12, 301 (1951), -C. Palache, D. Berman, C. Frondel.

34. L.J. Bhagia & J.R. Pandya. Indian Journal of Pure and Applied Physics, Vol 23, January 1985, 27.
35. N.S. Pandya & J.R. Pandya. Nature (Lond.) Sept. 19, 184, 894 (1959).
36. N.S. Pandya & J.R. Pandya. Journal M.S. University of Baroda (India). 09, No.2, 15 (1960).
37. N.S. Pandya & J.R. Pandya. Journal M.S. University of Baroda (India). 10, No.3, 21 (1961).
38. J.R. Pandya & R.T. Shah. Journal M.S. University of Baroda (India). 24, No.3, 41 (1975).
39. J.R. Pandya & B.J. Mehta. Min. Mag. (Lond.) 37, No.288, 526 (1969).
40. B.J. Mehta & J.R. Pandya. Surface Technology (Netherlands) 14, 139 (1981).
41. B.J. Mehta & J.R. Pandya. Surf. Tech. 14, 391 (1981).
42. B.J. Mehta & J.R. Pandya. Crystal Res. & Technol. 17, No.4, 485 (1982).
43. B.J. Mehta & J.R. Pandya, Surf. Tech. 15, 141 (1982).
44. B.J. Mehta, Surf. Tech. 11, (1980), 301.
45. B.J. Mehta, Surf. Tech. 12, (1981), 253.
46. B.J. Mehta, Surf. Tech. 13. 33 (1981).
47. B.J. Mehta, Indian Journal of Pure & Applied Physics, 19, No.12, 1206 (1981).
48. B.J. Mehta, Crystal Res. & Tech. 16, No.1, K16-18 (1981).
49. B.J. Mehta, Crystal Res. & Tech. 17, No.4, 481 (1982).
50. Bengusff, V.Z., Lavrentz, F.F., Soifer, L.M. and Startser, V.I., Soviet Phys. Crystallography. 5, 418 (1960)
51. Boos, A., Neues. Jb. Min., A78, 89 (1943)
52. Goldschmidt, V. and Porter, M.W., Beitr. Kryst. Min. 2, 138 (1924)
53. Himmel, H. & Kleber, W., Neues. Jb. Min. Geol. A72, 347 (1937)

54. Honess, A.P., The Nature, Origin and Interpretation of Etch Figures on Crystals. (John Wiley and Sons, Inc., N.Y.) (1927)
55. Honess, A.P. & Jones, J.R., Bull. Geol. Soc. Amer. 48, 667 (1937)
56. Ichikowa Shimmatsu, Am. J. Sci., 42, 111 (1916)
57. Keith, R.E. and Gilman, J.J., Acta Metall. 8, 1 (1960)
58. Kleber, W., Z. Krist. 102, 455 (1940)
59. Novak Jiri, Z. Krist. 90, 385 (1935)
60. Pfefferkorn, G., Optik, 7, 208 (1950)
61. Pfefferkorn, G., Fortschr. Min. 130, 34 (1951)
62. Pfefferkorn, G. and Westermann, H., Neues. Jb. Min. 5, 97 (1952)
63. Puchegger, F., Naturwiss, 39, 428 (1952)
64. Royer, L., Compt. Rend. 188, 1176 (1929)
65. Royer, L., Bull. Soc. Franc. Min. 53, 350 (1930)
66. Stanley, R.C., Nature (Lond.) 183, 1548 (1959)
67. Watts, H., Nature (Lond.) 183, 314 (1959)
68. E.C. Eckels, Cements, Limes & Plasters, Wiley New York, (1922)
69. N.V.S. Knibbs, Lime and Magnesia, E. Benn (Lond.)(1924)
70. A.B. Searle, Limestone & its products. their nature, production and uses, Ernest Benn Ltd. (London)(1935)
71. H.C. Bijawat & S.L. Sastry, High-Calcium Limestones of India, (1957), CSIR Publication, New Delhi.
72. R.S. Baynton, Chemistry & Technology of Lime and Limestones, Interscience Pub., New York, 1966.
73. A.J. Moses, The practising scientist's handbook - a guide for physical and terrestrial scientists and engineers. Van Nostrand Reinhold Company, New York (1978)

74. W.G. Driscoll, W. Vanaghan, Handbook of Optics, McGraw-Hill Book Company, New York (1978)
75. C. Palache, H. Berman, C. Frondel, "Dana's System of Mineralogy" 7th ed.(1951). John Wiley & Sons, Inc., (New York), Chapman and Hall Ltd., (London).
76. J.W. Mellor, A Comprehensive Treatise on Inorganic and Theoretical Chemistry, Longmans, Green and Co., New York (1923).
77. A.J. Shah, Ph.D. Thesis, M.S. University of Baroda, Baroda (1984)
78. Lange's Handbook of Chemistry, J.A. Dean (Editor), 11th ed. (1973). McGraw-Hill Book Company, New York.
79. F.A. Wade, R.B. Mattox, Elements of Crystallography and Mineralogy (1960), Oxford & IBH Publishing Co. (Calcutta).
80. A.R. Verma & O.N. Srivastava, Crystallography for Solid State Physics, Wiley Eastern Limited (1982)(New Delhi)
81. W.H. Brag & W.L. Brag, Proc. Roy. Soc. Lond., 89A, 246, (1914).
82. S. Tolansky & Khamasavi, Nature (London), 661, (1946)
83. C.V. Raman, Proc. Ind. Acad. Sci., A-48, 307, (1959).